

UNCERTAINTY QUANTIFICATION IN THE DYNAMIC RESPONSE OF ASSEMBLED STRUCTURES

E. Menga¹, C. López², S. Hernández², A. Baldomir², I. Romero³, M. J. Sánchez³

¹AIRBUS S.L.

Department of Loads and Aeroelasticity
A. John Lennon S/N, 28906 Getafe, Spain
edoardo.menga@airbus.com

²Structural Mechanics Group, School of Civil Engineering

Universidade da Coruña
Campus Elviña s/n, A Coruña 15071, Spain
carlos.lopez.rodriquez@udc.es
hernandez@udc.es

³ Mechanical Engineering Department, ETSI Industriales

Technical University of Madrid
José Gutiérrez Abascal, 2, 28006 Madrid, Spain
ignacio.romero@upm.es
mariajesus.sanchez@upm.es

Keywords: Uncertainty Quantification, Metamodel, Junctions, Structural Dynamics

Abstract:

This paper aims to review and explain fundamental tasks of the UQ process, particularly in the context of non-intrusive methods, which sample the deterministic model at points in the multidimensional input parameter space. Low Discrepancy Design (LDD) and Global Sensitivity Analysis (GSA) are shown to be effective analytical tools to define which parameters are relevant, the so-called Design Variables (DVs) and to quantify how the variance of the output is affected by the variance of the inputs. On the other side, especially for computationally expensive models, the direct use of the analytical model, i.e. Finite Element Model (FEM), can be extremely time-consuming. Hence, for complex systems, it is often necessary to generate first a meta-model and then, using it, complete the sensitivity analysis. The reliability and robustness of the method are demonstrated considering two structures with different level of complexity. In the first example the frequency response of a doble pinned beam is studied and discussed. In the second example the uncertain nonlinear vibrations of the RAM Air Inlet (RAI) system are considered. The stochastic reaction forces acting on the rods of the RAI mechanism are studied, considering prescribed density distributions on the interfaces, in terms of free-plays and stiffnesses, on the excitation force and on its dominant frequency. In this case the modal information is computed in NASTRAN and is translated to a MATLAB code, where the process is completed and the results evaluated. In both cases the relevant parameters are defined and the influence of each one on the variance of the output is clearly quantified. At the end of each example the results are discussed with a deep look at the physical coherence of the GSA Indices. Moreover, the second example gives the opportunity to discuss the use of Polynomial Chaos Expansion (PCE) meta-model in the frame of nonlinear vibration analysis.

1 INTRODUCTION TO UNCERTAINTY QUANTIFICATION (UQ)

Uncertainties Quantification can be defined as the science of identifying, quantifying and reducing uncertainties associated with the models, numerical implementations, experiments and quantities of interest.

Uncertainty Quantification (UQ) takes its bricks from classical statistics and numerical analysis theory, but they need to be included in a more systematic approach which takes into account the uncertainties of the inputs, how they are propagated through the model, which the output's density distributions and their statistical moments are, and, in a global sense, how sensitive the outputs are with respect the prescribed uncertain inputs. In this work the concept of UQ is explored in the frame of reliability and predictiveness of numerical models.

Assembled structures in aerospace industry are often connected thru discontinuous and nonlinear junctions whose mechanical properties are seldom well characterized experimentally. From a modeling point of view, they are often reduced to a set of linear springs with some stiffness values. At occurrence, during the project, these values are reviewed, argued and fine-tuned to get a reasonable or expected dynamic response. Local parameters are changed once-a-time to see at their effect on the outputs: the higher the number of input parameters, the more tedious the task is, as well, the more complex the understanding of the results. Interfaces are a key player in defining the dynamics of components and systems but considering properly their behavior can be a very complex task. This is especially true for dynamic studies. Their behavior is intrinsically uncertain and as consequence, it will make stochastic the dynamic response of the connected structures.

This work looks at the UQ process as a systematic approach to establish, quantitatively and qualitatively, how the uncertainties of the input parameters of a physical system are propagated to its outputs, focusing in the study of assembled structures. Some researchers have already investigated about considering uncertainty within the joints of assembled structures [1,2], as well as in the assembly and manufacture of certain structural applications such as micro-electromechanical systems [3].

UQ can be thought as a process with three fundamental phases, pre-processing, uncertainties propagation, post-processing, each of them including different tasks. Figure 1 shows schematically these three tasks and their breakdown, as well the data-flow within the process.

- *Pre-processing* phase requires the problem to be set-up, hence the uncertain inputs have to be selected and characterized, as well the Quantities of Interest, i.e. those outputs which provides information necessary to make conclusions or decisions about the process, have to be selected. Uncertain inputs can be represented by random variables. Classical categorization of uncertainties distinguishes between *aleatoric and epistemic uncertainties*. The former are associated to the inherent variation of the parameters, cannot be reduced by additional physical or experimental knowledge, but they can serve to better categorize the uncertainty from probabilistic point of view. The quantification of irreducible uncertainties pass by repeating experiments to establish a statistically significant sample. The latter refers to deficiencies that result from model assumptions, missing physics, lack of complete information about the system. These uncertainties are often biased and they are typically less naturally defined in a probabilistic framework. Anyway the distinction between aleatoric and epistemic uncertainties is not always clear since lack of knowledge is relative and depends on current theory and experimental capability. Often in UQ applications, epistemic uncertainties are reformulated as aleatoric, where probabilistic analysis

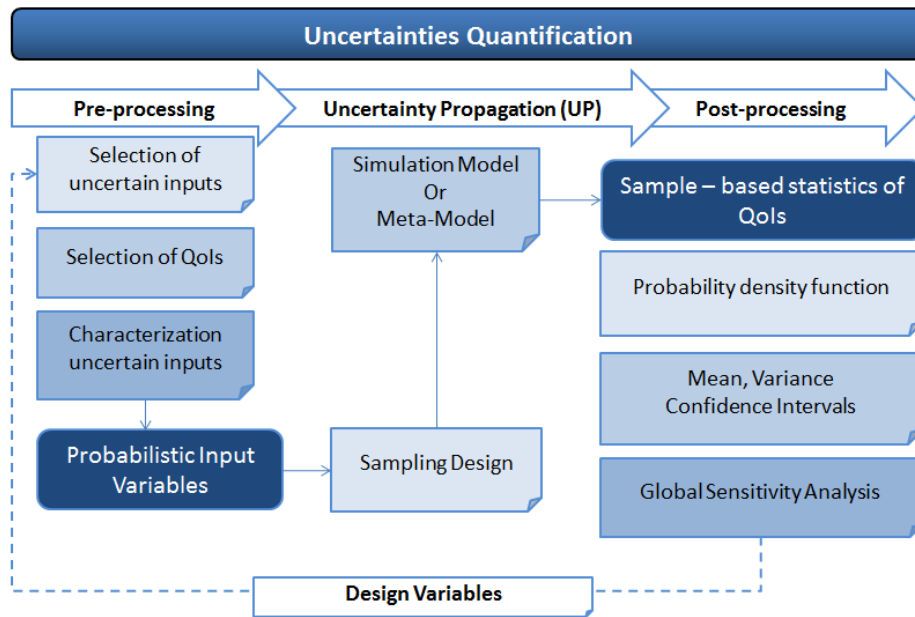


Figure 1: Uncertainty Quantification overview.

is applicable. It is often difficult to define an experimental-based probability distributions for all the uncertain inputs, and expert knowledge becomes fundamental. A common choice is exploring the model behavior assuming uniform distributions on the inputs, but it is worth to remark that changing the prescribed probabilities can lead to different conclusions and sometimes running analysis with several distributions and comparing the results can be a useful exercise.

In practice, the model can be seen as parametric system with certain probability distributions prescribed on selected input parameters.

- *Uncertain Propagation(UP)* characterizes the distribution of the QoIs for a given distribution of the inputs. Due to the uncertainty in the inputs, the outputs of the model become uncertain as well, but neither statistical moments nor a probability distribution are known a priori. They depend on the uncertainty of the parameters, which have to be propagated through the simulation. In the context of this work non-intrusive methods are considered. They are particularly attractive for complex-system because standard codes (i.e. FE programs) can be successfully used to model the response. Non-intrusive methods sample the deterministic model at points in the multidimensional input parameter space, according some specific sampling technique, to create a cloud of result points, which can be further post-processed to obtain sample-based statistics. The most common design is based on Monte Carlo Simulation (MCS), which relies on pure randomness. Due its randomness some points can be clustered closely, while other intervals within the space cannot get any samples. Hence, especially when working in high dimensions, most researchers seem to agree that generic, near-uniform, distribution of the data sites is a good strategy. Several sampling strategies try to cover this need, such as Latin Hypercube (LHD) and Low-Discrepancy Designs (LDD). Particularly, LDD generate a deterministic sequence of quasi-random numbers which allows one to fill uniformly a unit hypercube. In the context of this work the Sobol's LDD is considered. It has been found by several researchers, i.e. Pianosi in [4], out-performing the classical MCS and LHD, appearing, in the average, more efficient and with a faster convergence rate.

Anyway, when the computational demand of a single deterministic run is sufficiently high, sample-based approach based exclusively on the simulation model could be an unaffordable strategy. Hence, the need to first consider an efficient, smaller cloud of simulation points which allows to build a *meta-model*.

- *Post-processing* activities regard fundamentally the stochastic characterization of the QoIs, which means to provide the statistics of the output density distributions. As result of the UP, either directly by the simulation model or by a computational cheaper auxiliary meta-model, a sample-based cloud of output points is obtained. Therefore, during a post-processing step, the QoIs can be stochastically characterized, which means to provide sample-based estimates of the mean, variance and their confidence intervals. In this section we include also the *Global Sensitivity Analysis*, whose objective is to rank uncertain inputs according their influence on the outputs.

In the next sections a review of the Polynomial Chaos Expansion (PCE) meta-modeling and GSA concepts is done.

2 META-MODELING

For complex systems, where, possibly, a very large set of inputs is considered uncertain, it is often necessary to generate first a meta-model and then, using it, complete the UP.

Generation of a meta-model, or surrogate model, considers the computer simulations as a black-box which produces a set of outputs based on a given set of initial conditions and model parameters. The main task is to employ a scattered data fitting approach to produce a surrogate for such computer simulations. Compared with the original one, the meta-model, expressing the relationship between the QoIs and the input variables, is considered to be computationally inexpensive. Evidently, its generation requires a 'computer design', whose main objective is sampling the deterministic numerical model efficiently. That means to deal with the *curse of dimensionality*: the design should be able to effectively fill out the high-dimensional space and ensure an accurate solution of the scattered data fitting problem.

2.1 Meta-model: Polynomial Chaos Expansion

The original Hermite Polynomial Chaos Expansion (PCE), also known as homogeneous chaos, was first derived in [5] for the spectral representation of any stochastic response in terms of Gaussian random variables. Hermite polynomials are a subset of the hyper-geometrical polynomials, known as the Askey scheme [6], having orthogonal property with respect the gaussian probability density functions (PDF). In the study of [7] the method was extended under the Wiener-Askey scheme to others random distributions. In Table 1 the set of polynomials that provide an optimal basis for different Probability Density Functions (PDFs) is presented. Hence, in order to apply correctly the PCE approach, assuring optimal convergence properties, the polynomials are required to be orthogonal with respect a weight function, which is representative of the probability distribution of the QoIs. Really, the meta-model provides a fitting function of the QoIs densities.

In the finite dimensional random space Γ , the Hermite PCE for a response $Y(\mathbf{X})$, being \mathbf{X} a random variables vector, is an infinite polynomial expansion which in practice is truncated at a

| Orthogonal polynomial | Weight function | PDF | Density function |
|--------------------------------|----------------------|-------------|--|
| Hermite $H_e(x)$ | $e^{-\frac{x^2}{2}}$ | Normal | $\frac{1}{\sqrt{2\pi}}e^{-\frac{x^2}{2}}$ |
| Legendre $P_n(x)$ | 1 | Uniform | $\frac{1}{2}$ |
| Laguerre $L_n(x)$ | e^{-x} | Exponential | e^{-x} |
| Jacobi $P_n^{\alpha,\beta}(x)$ | $x^\alpha e^{-x}$ | Beta | $\frac{x^\alpha e^{-x}}{\Gamma(\alpha+1)}$ |

Table 1: Correspondence between orthogonal polynomials and PDF.

finite expansion order P as follows:

$$Y(\mathbf{X}) \cong \sum_{k=0}^P b_k \cdot \Psi_k(\mathbf{u}) \quad (1)$$

where b_k are unknown coefficients and Ψ_k are the Hermite polynomials evaluated in the *normalized* random variables vector \mathbf{u} . Hence the multivariate random variable \mathbf{X} has to be mapped in the domain where the orthogonality of the polynomials is ensured.

Usually, $\Psi_k(\mathbf{u})$ are multivariate polynomials that involve products of the one-dimensional polynomials $\psi_i(u_j)$, where i is the order of the polynomial ψ and u_j is the j component of the vector \mathbf{u} . Hence the expansion includes a complete basis of polynomials up to a fixed total-order specification P . The one-dimensional Hermite polynomials $\psi_i(u)$ are generally defined as:

$$\psi_i(u) = (-1)^i \cdot [\phi^{(i)}(u)/\phi(u)] \quad (2)$$

where $\phi^{(i)}(u)$ is the i th derivative of the PDF of the Normal distribution $N(0, 1)$, expressed as:

$$\phi(u) = (1/\sqrt{2\pi})exp(-u^2/2) \quad (3)$$

From Equation 2 the set of the i th order one-dimensional Hermite polynomials can be easily derived as:

$$\{\psi_i(u)\} = \{1, u, u^2 - 1, u^3 - 3u, u^4 - 6u^2 + 3, u^5 - 10u^3 + 15u, \dots\} \quad (4)$$

As an example, let's consider the multidimensional basis polynomials for a second-order expansion over two random variables:

$$\begin{aligned} \Psi_0(\mathbf{u}) &= \psi_0(u_1) \cdot \psi_0(u_2) = 1 \cdot 1 = 1 \\ \Psi_1(\mathbf{u}) &= \psi_1(u_1) \cdot \psi_0(u_2) = u_1 \cdot 1 = u_1 \\ \Psi_2(\mathbf{u}) &= \psi_0(u_1) \cdot \psi_1(u_2) = 1 \cdot u_2 = u_2 \\ \Psi_3(\mathbf{u}) &= \psi_2(u_1) \cdot \psi_0(u_2) = (u_1^2 - 1) \cdot 1 = u_1^2 - 1 \\ \Psi_4(\mathbf{u}) &= \psi_0(u_1) \cdot \psi_2(u_2) = 1 \cdot (u_2^2 - 1) = u_2^2 - 1 \\ \Psi_5(\mathbf{u}) &= \psi_1(u_1) \cdot \psi_1(u_2) = u_1 \cdot u_2 = u_1 u_2 \end{aligned}$$

The total number of coefficients N_c of the polynomial expansion of Equation 2 is given by:

$$N_c = \frac{(n+p)!}{n!p!} \quad (5)$$

where n is the number of random variables and p is the maximum order of the one-dimensional Hermite polynomials ψ . From this expression it can be noted that increasing the number of random variables or the order of the polynomial will cause a substantial grow in the number of terms N_c of the PCE. Hence this will imply an appreciable increase in the sample size and consequently in the computational burden associated for complex analyses. Therefore it is important to select carefully the random variables involved in order to spend a reasonable computational time.

There are several ways to estimate the unknown coefficients b_i of the PCE, for instance random sampling, tensor-product quadrature, Smolyak sparse grids or regression models. The first three approaches are spectral projection methods that consist of projecting the responses against each basis function using inner products, employing the orthogonal properties to extract the coefficients as a non-intrusive approach. Multiplying both sides of Equation 1 by $\Psi_j(\mathbf{u})$ and taking the expected values $\langle \cdot \rangle$, the following equation can be obtained:

$$\langle Y(\mathbf{X}) \cdot \Psi_j(\mathbf{u}) \rangle = \left\langle \sum_{k=0}^P b_k \Psi_k(\mathbf{u}) \Psi_j(\mathbf{u}) \right\rangle \quad (6)$$

Due to the orthogonality properties of the PCE, the coefficients can be obtained as:

$$b_k = \frac{\langle Y(\mathbf{X}) \cdot \Psi_k(\mathbf{u}) \rangle}{\langle \Psi_k^2(\mathbf{u}) \rangle} \quad (7)$$

From this expression, the denominator is evaluated analytically while the numerator requires a multi-dimensional integration, which can be accomplished through random sampling [8], Gaussian quadrature [9] or Smolyak sparse grids [10].

On the other hand, regression models (also known as stochastic response surfaces) may also be chosen. The order of the p polynomial expansion presented in Equation 1 can be expressed in matrix notation for N_s samples as follows:

$$\mathbf{Y} = \Psi \mathbf{b} + \mathbf{e} \quad (8)$$

where:

$$\mathbf{Y} = \begin{bmatrix} Y_1 \\ Y_2 \\ \vdots \\ Y_{N_s} \end{bmatrix}, \Psi = \begin{bmatrix} 1 & \Psi_1(u_1) & \dots & \Psi_p(u_1) \\ 1 & \Psi_1(u_2) & \dots & \Psi_p(u_2) \\ \vdots & \vdots & \ddots & \vdots \\ 1 & \Psi_1(u_{N_s}) & \dots & \Psi_p(u_{N_s}) \end{bmatrix}, \mathbf{b} = \begin{bmatrix} b_0 \\ b_1 \\ \vdots \\ b_p \end{bmatrix}, \mathbf{e} = \begin{bmatrix} e_1 \\ e_2 \\ \vdots \\ e_{N_s} \end{bmatrix} \quad (9)$$

and being \mathbf{e} the residuals. Usually, linear regression models use the method of least squares to obtain the unknown coefficients:

$$\mathbf{b} = (\Psi^T \Psi)^{-1} \Psi^T \mathbf{Y} \quad (10)$$

Once the coefficients are obtained, the fitted model $\hat{\mathbf{Y}}$ and the residuals can be expressed as:

$$\hat{\mathbf{Y}} = \Psi \mathbf{b} \quad e = \mathbf{Y} - \hat{\mathbf{Y}} \quad (11)$$

Sobol LDD is the sampling scheme selected since it is more efficient than the MCS method. The number of input points N_s must be higher than the number of unknown coefficients N_c , and depending on the complexity of the response the advisable number of samples may fluctuate. Hosder in its work [11] recommends $N_s = 2 \cdot N_c$.

3 VARIANCE BASED GLOBAL SENSITIVITY INDICES

GSA defines a qualitative and quantitative mapping between the input variables and the Quantities of Interest (QoIs). Sensitivity analysis are strictly related to the UP and they can be seen as complementary to each other: UP quantifying the uncertainty in the output of the model, while GSA focuses on apportioning output's uncertainty to the different sources of uncertain parameters.

A. Saltelli, M. Ratto [12] give the following definition of sensitivity analysis (SA): "*the study of how uncertainty in the output of a model (numerical or otherwise) can be apportioned by different sources in the model input*", where the concept of sensitivity analysis is explicitly included in the process of uncertainty quantification. So, GSA not just allows to select what the relevant parameters in the model are, but are able to score the different parameter according their relevance in the QoIs. In this context, a sensitivity index is a measure of the influence of an uncertain quantity on an output variable.

Most popular GSA techniques are based on the decomposition of variance's output probability distribution. These techniques rely on three basic principles:

- the uncertainty of input parameters is described by their probability density function and therefore that induces a probability distribution of the output;
- the variance of the output probability distribution is a good indicator of output's uncertainty;
- the contribution of an input parameter, to the output's variance, is a measure of sensitivity.

GSA allows the calculation of the Sobol' Sensitivity Indexes. They refer to Sobol, because the decomposition of the variance can be formulated analytically from the High Dimensional Model Representation (HDMR) of Sobol [13]. From a practical point of view, particular interest is deserved to the *first order* and *total order sensitivity indices*, respectively S_i^I and S_i^T , also called *main effects* and *total effects*.

Main effects represent the measure of the contribution of the parameter X_i to the output variance, or equivalently, the expected percentage reduction of the output variance $V(Y)$ obtained when the uncertainty of input parameter X_i is eliminated.

$$S_i^I = \frac{V_{X_i}[E_{X_{\sim i}}(Y | X_i)]}{V(Y)} = \frac{V(Y) - E_{X_i}[V_{X_{\sim i}}(Y | X_i)]}{V(Y)}. \quad (12)$$

Total effects represent the total contribution of an input parameter considering its individual effect and its interactions with all the other factors:

$$S_i^T = \frac{E_{X \sim i}[V_{X_i}(Y | X_i)]}{V(Y)} = \frac{V(Y) - V_{X \sim i}[E_{X_i}(Y | X_i)]}{V(Y)}. \quad (13)$$

The popularity of the main and total effects is also due to the relatively easy algorithms, mostly proposed by Saltelli, which provide sample-based close-form equations for their approximation. A very good review of sample-based estimators is given in Saltelli and Annoni [14].

However, the sample size, hence the number of runs, required to achieve reliable values of the first and total indices estimators, can be rather large, which makes the direct application of these approaches quite unthinkable for time-consuming models. Hence, methods for reducing the computational burn have arisen. The most widely used are those based on the Fourier Amplitude Sensitivity Test (FAST) and those based on meta-modelling. FAST was first developed by Cukier in 1973 [15] for estimating the main effects and further extended (E-FAST) to the total effects by Saltelli in 1999 [16]. Meta-modelling plays also an important role, because a limited set of runs is supposed to be sufficient for building a surrogate of the original model, and then this, computationally inexpensive, is used to complete the GSA.

Moreover, GSA can be seen as a sort of dimension reduction tool and once the set of relevant parameters is selected, one can think to generate a more refined UQ process (UP, Meta-modelling, etc...) but only including those variables having the most significant impact on the response. Parameters belonging to this smaller set are often called Design Variables (DVs). Out of the scope of this work, but it is evident the benefit of such approach in Design Optimization.

4 POLYNOMIAL CHAOS AND SOBOL'S INDICES

According to the PCE theory, the mean and the variance of the QoIs can be estimated directly by mean of the PCE coefficients. In fact, assuming the polynomials normalized to the variance, the following relationships hold:

$$E(Y(X)) \approx b_0 \quad (14)$$

$$V(Y(X)) \approx \sum_{m=1}^p b_m^2 \quad (15)$$

With reference to the bivariate polynomial of second order considered in paragraph 2.1, table 2 shows as the univariate are combined by the use of a multi-index α_k and the regression coefficients.

It is straightforward to see a close similarity between the PCE and the High Dimensional Model Reduction (HDMR) proposed by Sobol. In fact, the output functions can be seen as the sum of higher dimensional terms defined according to the multi-index α_k . In addition the Sobol's condition for the uniqueness of the decomposition requires expressing the output function as the summation of a constant term plus higher dimensional zero-mean function. Condition satisfied thanks to the polynomials orthogonality. In case of two input variables, the Sobol's HDMR, is:

$$Y(\mathbf{X}) = f(X_1, X_2) = f_0 + f_1(X_1) + f_2(X_2) + f_{12}(X_1, X_2) \quad (16)$$

| Polynomial Chaos Expansion 2nd order | | | | |
|--------------------------------------|-------------|--------------|---|-------|
| Multivariate PCE | Multi-Index | Coefficients | | |
| $\Psi_0(\mathbf{u})$ | α_0 | 0 | 0 | b_0 |
| $\Psi_1(\mathbf{u})$ | α_1 | 1 | 0 | b_1 |
| $\Psi_2(\mathbf{u})$ | α_2 | 0 | 1 | b_2 |
| $\Psi_3(\mathbf{u})$ | α_3 | 2 | 0 | b_3 |
| $\Psi_4(\mathbf{u})$ | α_4 | 0 | 2 | b_4 |
| $\Psi_5(\mathbf{u})$ | α_5 | 1 | 1 | b_5 |

Table 2: Bivariate PCE of 2^{nd} order - coefficients.

$$\hat{Y}(\mathbf{X}) = b_0 + b_1\psi_1(u_1) + b_2\psi_1(u_2) + b_3\psi_2(u_1) + b_4\psi_2(u_2) + b_5\psi_1(u_1)\psi_1(u_2) \quad (17)$$

In the example b_0 defines the constant term, the sum of polynomials Ψ_1 and Ψ_3 , defined by α_1 and α_3 give the $f_1(u_1) = b_1\psi_1(u_1) + b_3\psi_2(u_1)$, as well $f_{12}(u_1, u_2) = b_5\psi_1(u_1)\psi_1(u_2)$. Hence the total variance, defined by equation 15 can be decomposed as:

$$V(Y) = V(f_0) + V(f_1) + V(f_2) + V(f_{12}) \quad (18)$$

where the explicit dependence of each function from its variables has been omitted for a matter of compactness and readability.

Again referencing to table 2, the f_0 is a constant term and has a variance zero, the contribution to the total variance due to the function $f_1(X_1)$ is $V(f_1) = b_1^2 + b_3^2$, as well $V(f_{12}) = b_5^2$, and so on. The Sobol's indices can be gotten by the ratio between the partial variances and the total one. For example the first and total effects within the first input variable X_1 are:

$$S_1^I = \frac{V(f_1)}{V(Y)} \approx \frac{b_1^2 + b_3^2}{\sum_{m=1}^p b_m^2} \quad (19)$$

$$S_1^T = \frac{V(f_1) + V(f_{12})}{V(Y)} \approx \frac{b_1^2 + b_3^2 + b_5^2}{\sum_{m=1}^p b_m^2} \quad (20)$$

Hence the calculation of the PCE coefficients provides a straightforward and computational cheap way to estimate the mean, the variance and the variance based indices. The reliability of this estimation is as good as the assumption made for constructing the meta-model, particularly in terms of degree of univariate polynomials and degree chosen for the truncation of the multivariate expansion.

5 APPLICATION EXAMPLES

5.1 Double pinned beam

The first example is a structural scheme formed by two built-in cantilever beams of 1000 mm which are connected by two sets of springs in x,y and xy directions at points *node1*, *node2*. The material is aluminum with a Young's module of $E_{al} = 70000[MPa]$ and a density of $\rho_{al} = 2.7e^{-9}[t/mm^2]$. Details are in table 3. The modal damping of the structure is assumed to

be 0.02 for all the modes. The load is defined as an harmonic sinus load $p = 1 \cdot \sin(\omega t)$ applied in vertical direction at the dynamic point defined by $DP1$. The response of the structure is evaluated at the response point : $RP1$. A detailed scheme of the two-bar two-strings structure is presented in Figure 2.

| Length [mm] | Young Module [MPa] | Density [t/mm ³] | Area[mm ²] | Inertia [mm ⁴] |
|-------------|--------------------|------------------------------|------------------------|----------------------------|
| 1000 | 70000 | $2.7e^{-9}$ | 1600 | $0.7e^4$ |

Table 3: Beams' properties.

The random variables are the springs' stiffnesses K_{1x}, K_{1y}, K_{1xy} and K_{2x}, K_{2y}, K_{2xy} , respectively for the first and second connection. We want the study the variability of the first peak of vibration when on the springs' stiffnesses a uniform distribution, with a possible variation of a 30% with respect to the nominal values, is prescribed. The nominal value is assumed to be the same for all the springs: $K_{nom} = 100[N/mm]$. Two QoIs are considered: the magnitude of the peak and the frequency at which the peak happens.

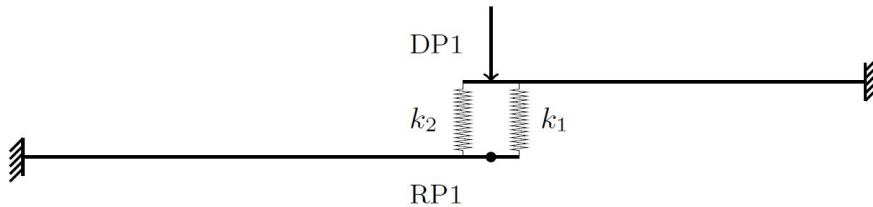


Figure 2: Two-bar structure

| Random Variable x | Distribution | nominal | lower bound | upper bound |
|---------------------|--------------|---------|-------------|-------------|
| K_{1x} [N/mm] | Uniform | 100 | 70 | 130 |
| K_{1y} [N/mm] | Uniform | 100 | 70 | 130 |
| K_{1xy} [N/mm] | Uniform | 100 | 70 | 130 |
| K_{2x} [N/mm] | Uniform | 100 | 70 | 130 |
| K_{2y} [N/mm] | Uniform | 100 | 70 | 130 |
| K_{2xy} [N/mm] | Uniform | 100 | 70 | 130 |

Table 4: Statistical moments of the random variables.

A multivariate 2^{nd} order PCE is used to build the meta-model up. According the table 1 univariate Legendre polynomials are employed for the uniform distributed variables. Table 5 shows the multivariate Legendre PCE of 2^{nd} order. The number of the regression coefficients is $N_c = 28$ and consequently the number of samples should be about $N_s = 60$. A convenient form to implement the polynomials in a code is the use of the so called *three-terms-relationship*. The interest reader can find more detail for example in [17]. A convenient way of using these polynomials requires their normalization with respect the variance. This is obtained dividing the each basis function for the square root of its variance.

For testing purpose 400 simulations are run, 60 of them are used as training set in order to obtain the coefficients of the expansion, the remaining part is later used as evaluation set in order to estimate the error, which is defined as:

| Multi-Index α_k | Multivariate Basis Function Ψ_k | Mean $E(\Psi_k)$ | Variance $V(\Psi_k)$ |
|------------------------|--------------------------------------|------------------|----------------------|
| $\alpha_0 = [0 \ 0]$ | $\Psi_0 = 1$ | 1 | $V(\Psi_0) = 1$ |
| $\alpha_1 = [1 \ 0]$ | $\Psi_1 = u_1$ | 0 | $V(\Psi_1) = 1/3$ |
| $\alpha_2 = [0 \ 1]$ | $\Psi_2 = u_2$ | 0 | $V(\Psi_2) = 1/3$ |
| $\alpha_3 = [2 \ 0]$ | $\Psi_3 = (3u_1^2 - 1)/2$ | 0 | $V(\Psi_3) = 1/5$ |
| $\alpha_4 = [0 \ 2]$ | $\Psi_4 = (3u_2^2 - 1)/2$ | 0 | $V(\Psi_4) = 1/5$ |
| $\alpha_5 = [1 \ 1]$ | $\Psi_5 = u_1 \cdot u_2$ | 0 | $V(\Psi_5) = 1/9$ |

Table 5: Multivariate Legendre Polynomials

$$Err = \frac{\|Y_{ev} - \Psi_{ev} \cdot b\|}{N_{s,ev} \|\Psi_{ev} \cdot b\|} \quad (21)$$

Figure 3 shows the variability of the first frequency response of the beam over the variability of the spring stiffnesses, and details the cloud of peak points, where the red points represent the results from the hard runs while the green ones, those coming from the PCE. The PCE meta-model, extremely cheap, constructed with a limited set of 60 output points, get a good fit over the remaining 340. The error obtained for the peak of the response is $1.572e^{-7}$, and for the frequency is $8.975e^{-8}$. The sample-based density distributions of the QoIs can be obtained with a wider sample by mean of the meta-model. They are showed in figure 4.

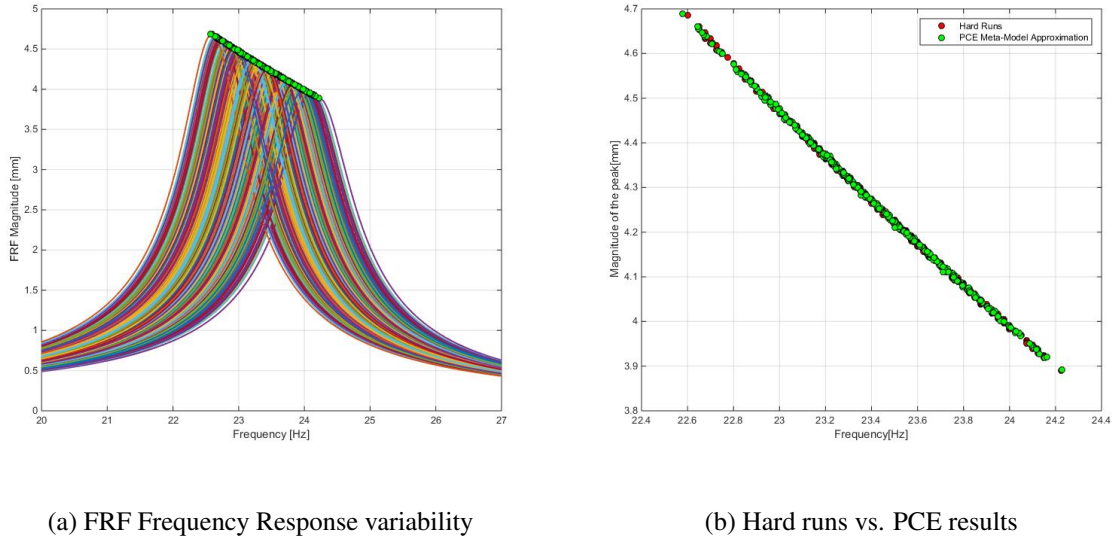
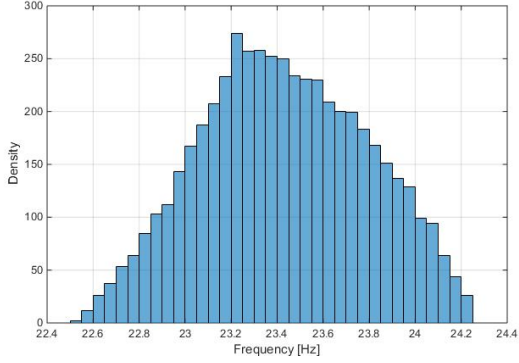


Figure 3: Stochastic output response.

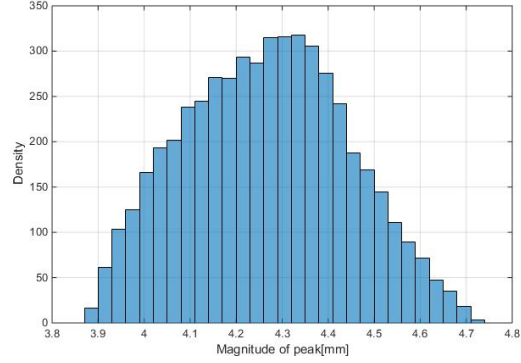
Finally we consider the calculation of the Sobol's Indices according the procedure described in paragraph 4. First, the regression coefficients of the PCE are obtained (see Table 6). Then the results of Sobol's Indices are presented in table 7: mean, variance, first and total orders. They are fully coherent with the physics of the problem. In fact the only springs' stiffness values affecting the response are K_{1y} and K_{2y} , moreover, the values of the sensitivity indices S_2 and S_5 , regarding these parameters, are the same because the problem is completely symmetric. Also, the first and total order are the same, which again is coherent with the expectation of not having any interactions among the parameters.

| PCE Coefficient | Frequency[Hz] | Peak[mm] | Multi-Index | | | | | |
|-----------------|---------------|-----------|--------------|--------------|--------------|--------------|--------------|--------------|
| | | | $\psi_i(u1)$ | $\psi_i(u2)$ | $\psi_i(u3)$ | $\psi_i(u4)$ | $\psi_i(u5)$ | $\psi_i(u6)$ |
| b_0 | 2.34E+01 | 4.27E+00 | 0 | 0 | 0 | 0 | 0 | 0 |
| b_1 | 2.78E-04 | 4.90E-04 | 1 | 0 | 0 | 0 | 0 | 0 |
| b_2 | -5.42E-04 | -2.02E-04 | 2 | 0 | 0 | 0 | 0 | 0 |
| b_3 | 2.53E-01 | -1.23E-01 | 0 | 1 | 0 | 0 | 0 | 0 |
| b_4 | -2.76E-02 | -7.05E-04 | 0 | 2 | 0 | 0 | 0 | 0 |
| b_5 | -4.39E-04 | 1.51E-02 | 0 | 0 | 1 | 0 | 0 | 0 |
| b_6 | 2.50E-04 | 8.44E-05 | 0 | 0 | 2 | 0 | 0 | 0 |
| b_7 | 3.21E-04 | -3.64E-04 | 0 | 0 | 0 | 1 | 0 | 0 |
| b_8 | 8.61E-04 | -3.35E-04 | 0 | 0 | 0 | 2 | 0 | 0 |
| b_9 | 2.54E-01 | -6.05E-04 | 0 | 0 | 0 | 0 | 1 | 0 |
| b_{10} | -2.77E-02 | 4.06E-04 | 0 | 0 | 0 | 0 | 2 | 0 |
| b_{11} | -8.61E-04 | -1.85E-04 | 0 | 0 | 0 | 0 | 0 | 1 |
| b_{12} | 2.63E-04 | -4.78E-07 | 0 | 0 | 0 | 0 | 0 | 2 |
| b_{13} | -7.38E-04 | 4.43E-04 | 1 | 1 | 0 | 0 | 0 | 0 |
| b_{14} | 3.03E-05 | -4.85E-04 | 1 | 0 | 1 | 0 | 0 | 0 |
| b_{15} | -4.59E-04 | -1.23E-01 | 1 | 0 | 0 | 1 | 0 | 0 |
| b_{16} | 4.31E-04 | -5.77E-05 | 1 | 0 | 0 | 0 | 1 | 0 |
| b_{17} | 7.99E-04 | -9.69E-03 | 1 | 0 | 0 | 0 | 0 | 1 |
| b_{18} | 6.67E-04 | -4.91E-05 | 0 | 1 | 1 | 0 | 0 | 0 |
| b_{19} | -1.09E-03 | -4.25E-04 | 0 | 1 | 0 | 1 | 0 | 0 |
| b_{20} | 2.76E-02 | 1.51E-02 | 0 | 1 | 0 | 0 | 1 | 0 |
| b_{21} | -8.18E-05 | 1.04E-04 | 0 | 1 | 0 | 0 | 0 | 1 |
| b_{22} | 1.06E-03 | -1.59E-06 | 0 | 0 | 1 | 1 | 0 | 0 |
| b_{23} | -1.18E-03 | 2.55E-04 | 0 | 0 | 1 | 0 | 1 | 0 |
| b_{24} | -1.08E-03 | -2.92E-04 | 0 | 0 | 1 | 0 | 0 | 1 |
| b_{25} | 1.88E-04 | -2.75E-05 | 0 | 0 | 0 | 1 | 1 | 0 |
| b_{26} | 8.93E-04 | -3.42E-04 | 0 | 0 | 0 | 1 | 0 | 1 |
| b_{27} | 6.63E-04 | -2.35E-04 | 0 | 0 | 0 | 0 | 1 | 1 |

Table 6: Regression Coefficients and Multi-Index



(a) Histogram of the frequency



(b) Histogram of the peak magnitude

Figure 4: Histogram of the frequency and peak magnitude.

| Parameter | Results | Frequency | Peak |
|-----------|---------|-----------|------|
| | Mean(Y) | 23.42 | 4.27 |
| | V(Y) | 0.13 | 0.03 |
| K_{1x} | S_1 | 0.00 | 0.00 |
| K_{1y} | S_2 | 0.50 | 0.50 |
| K_{1xy} | S_3 | 0.00 | 0.00 |
| K_{2x} | S_4 | 0.00 | 0.00 |
| K_{2y} | S_5 | 0.50 | 0.50 |
| K_{2xy} | S_6 | 0.00 | 0.00 |
| K_{1x} | ST_1 | 0.00 | 0.00 |
| K_{1y} | ST_2 | 0.50 | 0.50 |
| K_{1xy} | ST_3 | 0.00 | 0.00 |
| K_{2x} | ST_4 | 0.00 | 0.00 |
| K_{2y} | ST_5 | 0.50 | 0.50 |
| K_{2xy} | ST_6 | 0.00 | 0.00 |

Table 7: Double pinned beam - statistical moments and Sobol's Indices.

5.2 A380 RAM Air Inlet free-play nonlinear vibrations

In this section the UQ is considered in the frame of a much more complex case: A380 RAM Air Inlet nonlinear vibrations. First we define the Air Generation Unit (AGU), which is the system to supply and maintain the air in the pressurized fuselage compartments at the correct pressure, temperature and freshness for passenger comfort and equipment cooling where required. The System also provides air for ventilation functions in the un-pressurized fuselage bays. The AGU is connected to the ambient air by the RAM Air Inlet. The RAM is a moving part in a machine which puts pressure or force on something. The RAM Air Inlet(RAI) - RAM Air Outlet(RAO) openings modulating provides a forced ventilation system to control air temperature around the AGU.

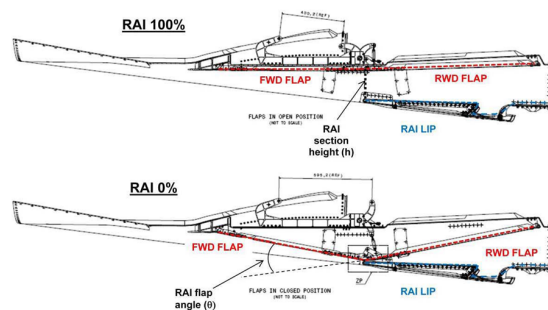
With reference to figure 5(a), we can see the left hand A380 air intake of the RAI and two outtakes of the RAO. Figure 5(b) shows the RAI system. The air flow, coming from the RAI intake, wets the forward and progressively the rearward flaps, passes towards the heat exchange and finally, goes out through the RAO outtakes. The RAI forward(FWD) and rearward(RWD) flaps are two moving panels whose relative position defines the variable RAI section height, hence the amount of air needed for the heat exchange. In the figure two extreme positions are showed: the maximum opening (RAI 100%) and the minimum one (RAI 0%). An actuator, through a kinematic chain, adjusts the flaps position. Figure 6 shows the mechanism. During flights, for a fixed actuator position, due to the flow acting on the flaps, particular attention is required in order to evaluate the forces explicated on the two rods, which connect, the RWD flap to the shaft.

Large flight test campaign has facilitate the individuation of the worst case in term of flaps positions and pressure loads distributions, but the evaluation of these forces is further complicated by :

- the free-plays between the arms and the rods at their interfaces, which make the response of the system strongly nonlinear;
- the uncertainties about the gaps sizes and the rods stiffnesses;
- the uncertainties about the magnitude of the resultant forces on the flaps and their dominant frequency.



(a) A380 RAI intake and RAO outtakes



(b) A380 RAI System flaps

Figure 5: A380 - RAM Air Inlet.

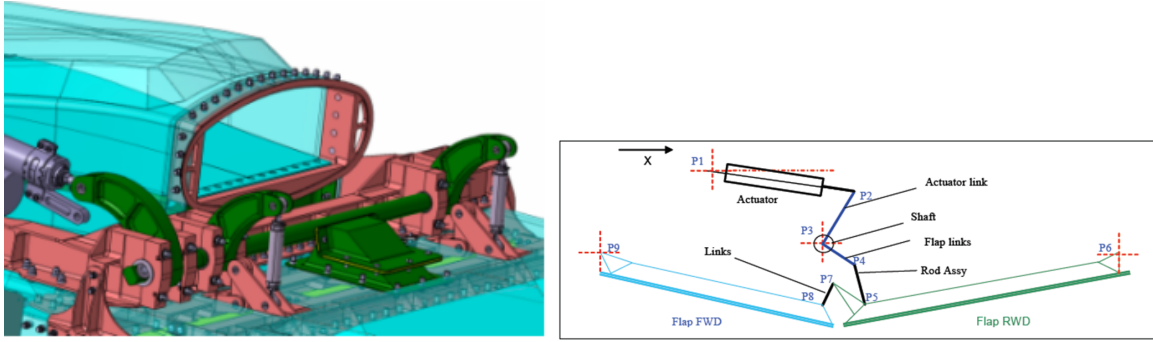


Figure 6: RAM Air Inlet - kinematic of flaps control.

This UQ process is used to estimate the density distributions of two QoIs: the root mean square of the nonlinear reaction forces acting on the two rods (i.e $F1_{rms}$ and $F2_{rms}$). The RMS is estimated for each run over a time period of 10 [sec]. The deterministic model is sampled according a Sobol's LDD of size $N_{run} = 400$, which could be already a very expensive computational cost considering the time required by the model due to the nonlinearities. This initial cost has been considerably reduced by the use of ANFRA (Advanced Nonlinear Frequency Response Analysis), which is a tool developed at Component Loads and Component Dynamics Department of Airbus Spain in conjunction with the Structural Mechanics Group of Universidade da Coruña. The ANFRA is based on a high efficient and improved version of the Structural Dynamic Modification Method (SDMM) but extended to nonlinear modifications. The methodology allows to obtain the nonlinear response updating the baseline modal base according the prescribed set of modifications, hence the eigenvalue problem has to be solved just once. The interest reader can refer to the works in [18–20], as well to the paper presented in this IFASD-2017-93 [21]. The baseline spectral matrix is obtained in NASTRAN from the FE Model showed in figure 7, with the rods disconnected from their arms. The reliability and robustness of the ANFRA approach can be seen in figure 8, where the response obtained updating the disconnected modal base (red line) fits perfectly the NASTRAN response of the connected structure.

The nonlinear modifications consider an uncertain free-play stiffness as shown in figure 9(a). On each rod the size of the gap and the stiffness are considered as random variable with prescribed normal distribution. Additionally, as shown in table 8 uniform distributions are considered on the force exciting the RWD Flap and its dominant frequency. Figure 9(b) shows the comparison between the linear force and the nonlinear one on the right rod, when the model is at its nominal conditions.

| Random Variable x | Distribution | nominal | lower bound | upper bound |
|---------------------|--------------|------------|--------------------|-------------|
| Force [N] | Uniform | 500 | 350 | 650 |
| Frequency [Hz] | Uniform | 35 | 29.5 | 40.5 |
| Random Variable x | Distribution | mean value | standard deviation | |
| K_1 [N/mm] | Normal | $1.5e^4$ | $1.5e^3$ | |
| K_2 [N/mm] | Normal | $1.5e^4$ | $1.5e^3$ | |
| Gap_1 [mm] | Normal | 1.5 | 0.3 | |
| Gap_2 [mm] | Normal | 1.5 | 0.3 | |

Table 8: Statistical distributions of the random variables.

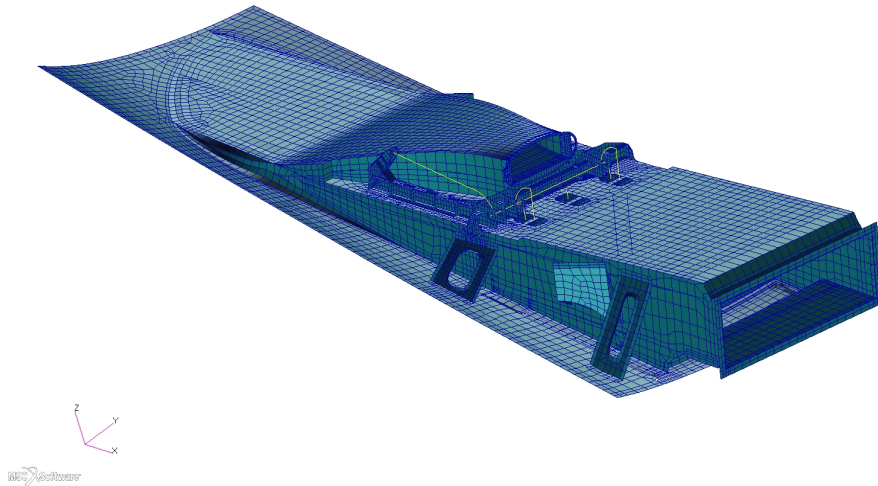
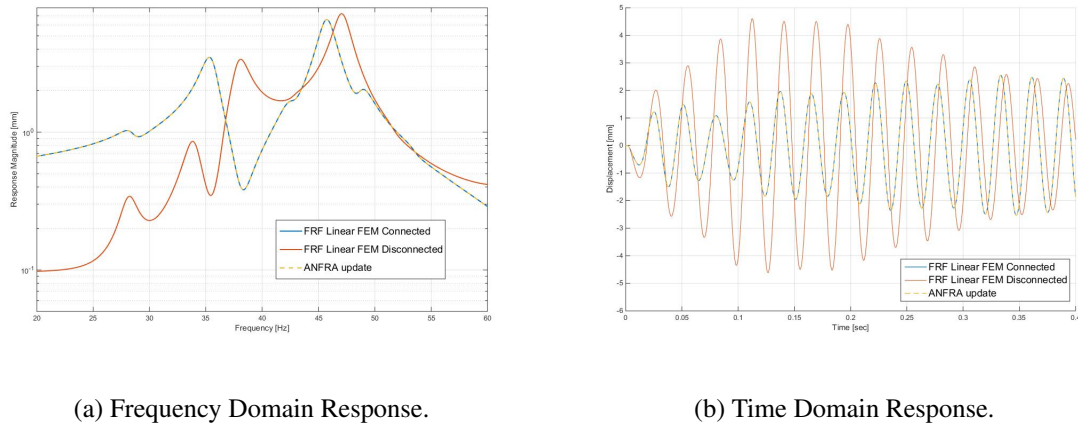


Figure 7: RAI FE Model



(a) Frequency Domain Response.

(b) Time Domain Response.

Figure 8: ANFRA updating method vs. NASTRAN.

The results are obtained through a 3^{rd} order PCE using a sample of $N_s = 250$, the remaining $N_{eval} = N_{run} - N_s = 150$ is used as evaluation set for estimating the error. The multivariate PCE takes into account univariate Legendre polynomials for the uniform distributions, as well Hermite polynomials for the normal ones. The independence of the random variable preserves the orthogonality of the multivariate PCE when different types of polynomials are used. The obtained error is of the order 10^{-3} . Which is several order of magnitude higher than in the previous example. Usually, PCE shows lower performance in case of strong nonlinearities, and increasing de degree of the multivariate polynomial helps until a certain point because due to the well-known Gibbs phenomenon over-fitting issues arise. On the other side, the higher the degree, the higher the number of the regression coefficients and the sample needed for the fitting are. In this open field of research other types of meta-models could better perform in case of strong nonlinear problems.

Table 9 shows the first two statistical moments, the error on the evaluation set and the variance based sensitivity indices. The frequency in accordance with the select range of variability has the stronger contribution, in fact, looking at figure 8, both the intact and disconnect structures

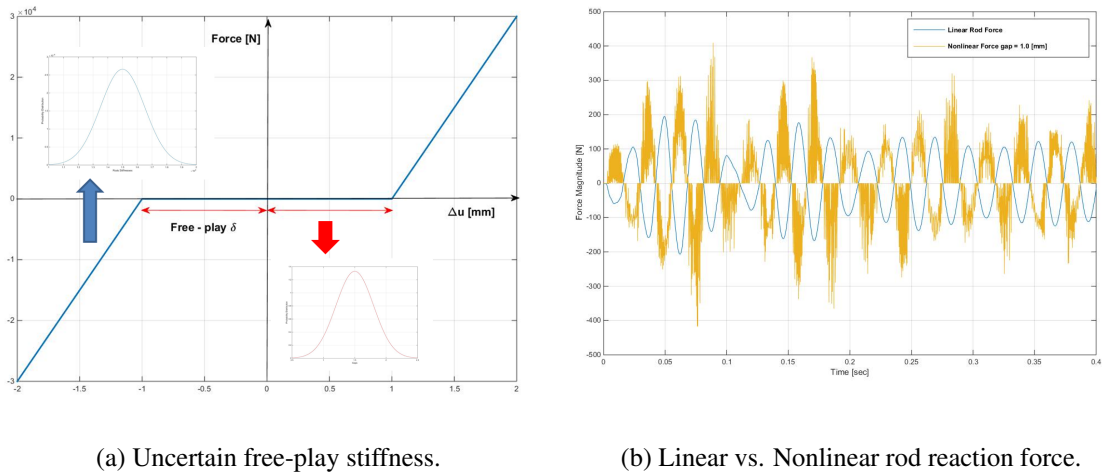


Figure 9: Nonlinear interfaces behavior.

present amplification peaks. The stiffnesses have the lowest contributions, which is expected as well having the nonlinearity due the free-play a much stronger effect on the reaction loads. Looking at the table, differences can be seen between the first and total order effects, which means that the interaction among parameters is significant. It is particularly true for the total indices regarding the gap parameters. It makes sense because interactions are expected at least between the applied force and the gap, hence for example the $ST_5 = S_5 + S_{15} + S_{25} + S_{35} + S_{45} + S_{65}$ is physically expected to have at least the term S_{15} different from zero. In figure 10 the split of the $F1_{rms}$ output variance among the input uncertain parameter is presented by pie plots. It is worth to note that when the interaction factors are significant the sum of the first order indices is less than one, hence the pie plot does not cover the 100% of the total variance. On the contrary the sum of the total effects can be greater than one, because for example the factor S_{15} contributes to both ST_5 and ST_1 , hence the percentages in the total effects pie plot are redistributed according the value of their sum.

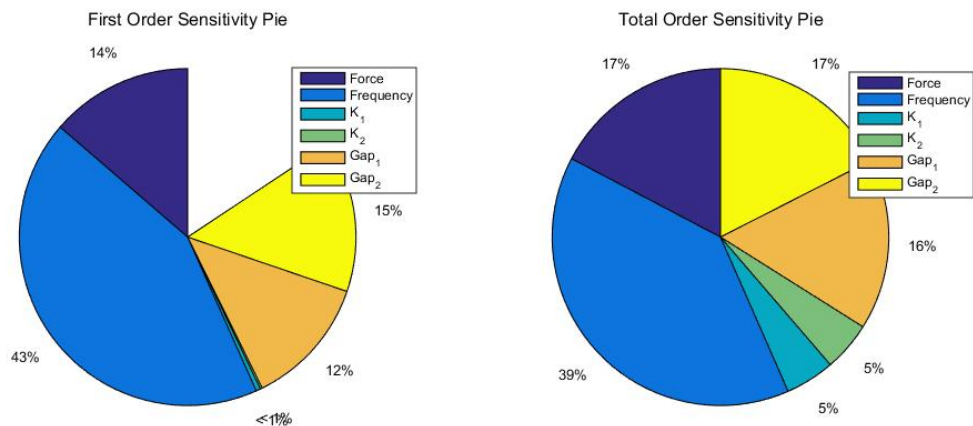


Figure 10: Reaction force $F1_{rms}$ - Total Variance Pie according the first and total indices.

| Parameter | Results | $F1_{rms}$ | $F2_{rms}$ |
|------------------|---------------------------------------|------------|------------|
| | Mean(Y) | 140.10 | 207.49 |
| | V(Y) | 3286.55 | 8145.43 |
| | error on N_{eval} | 0.0015 | 0.0024 |
| <i>Force</i> | S_1 | 0.14 | 0.17 |
| <i>Frequency</i> | S_2 | 0.43 | 0.30 |
| K_1 | S_3 | 0.00 | 0.01 |
| K_2 | S_4 | 0.00 | 0.01 |
| Gap_1 | S_5 | 0.12 | 0.17 |
| Gap_2 | S_6 | 0.15 | 0.06 |
| <i>Force</i> | ST_1 | 0.21 | 0.28 |
| <i>Frequency</i> | ST_2 | 0.48 | 0.38 |
| K_1 | ST_3 | 0.06 | 0.10 |
| K_2 | ST_4 | 0.06 | 0.09 |
| Gap_1 | ST_5 | 0.20 | 0.27 |
| Gap_2 | ST_6 | 0.22 | 0.21 |

Table 9: RAI vibrations - statistical moments and Sobol's Indices.

6 CONCLUSIONS

This research presents the UQ process as a systematic approach to estimate the probabilistic dynamic response of structures. Particular focus is put on the generation of PCE meta-models, which allows to describe the probability density function of the QoIs, as well facilitates the estimation of the Sobol's Sensitivity Indices. GSA are shown to be a fundamental and reliable tool for understanding which the relevant parameters are and how their variance contribute to the total variance of the outputs. The paper presents the key points of the theory behind the work but tries to make them fluent and easy to follow for the reader. Then the work is contextualized in the frame of assembled structure, whose interfaces, often having a nonlinear behavior, are a well-known source of uncertainties. Two example with different degree of complexity are presented. The first, a double pinned beam, is used as step-by-step guidance for the interested reader, who can reproduce easily the results by himself. The second, the nonlinear free play vibrations of the RAI system, is much more complex as well, much more interesting. The results, particularly regarding the first and total order effects, are discussed looking at their physical coherence and some perspective on the use of PCE in case of nonlinear problems is given.

7 REFERENCES

- [1] Gangadharan, S. and Nikoladaidis, E. (1991). Probabilistic system identification of two flexible joint models. *AIAA Journal*, 29(8), 1319–1326.
- [2] Walther, H. and Kmetyk, L. (2004). Bolted joints: Model uncertainty vs. test variability. *Proceedings of the 22nd IMAC, Dearborn, Michigan, (USA)*.
- [3] Kladitis, P., Bright, V., and Kharoufeh, J. (2004). Uncertainty in manufacture and assembly of multiple-joint solder self-assembled microelectromechanical systems (mems). *Journal of Manufacturing Processes*, 6(1), 32–50.

- [4] Pianosi, F., Beven, K., Freer, J., et al. (2016). Sensitivity analysis of environmental models: A systematic review with practical workflow. *Environmental Modelling & Software*, 79, 214–232.
- [5] Wiener, N. (1938). The homogeneous chaos. *American Journal of Mathematics*, 60(4), 897–936.
- [6] Askey, R. and Wilson, J. (1985). Some basic hypergeometric polynomials that generalize jacobi polynomials. *Memoirs of the American Mathematical Society* 319, AMS, Providence, RI.
- [7] Xiu, D. and Karniadakis, G. E. (2003). The Wiener-Askey polynomial chaos for stochastic differential equations. *SIAM Journal of Scientific Computing*, 187, 137–167.
- [8] Field, R. (2002). Numerical methods to estimate the coefficients of the polynomial chaos expansion. *Proceedings of the 15th ASCE engineering mechanics conference*.
- [9] Le Maître, O. and Knio, O. M. (2010). *Spectral methods for uncertainty quantification: with applications to computational fluid dynamics*. Springer Science & Business Media.
- [10] Smolyak, S. (1963). Quadrature and interpolation formulas for tensor products of certain classes of functions. *Sov. Math. Dokl.*, (4), 240–243.
- [11] Hosder, S., Walters, R., and Balch, M. (2007). Efficient sampling for non-intrusive polynomial chaos applications with multiple uncertain input variables. *Proceedings of the 48th AIAA/ASME/ASCE/AHS/ASC Structures, Structural Dynamics, and Materials Conference, No. AIAA-2007-1939, Honolulu, HI, April 2326*.
- [12] Saltelli, A., Ratto, M., Andres, T., et al. (2008). *Global sensitivity analysis: the primer*. John Wiley & Sons.
- [13] Sobol, I. M. (2003). Theorems and examples on high dimensional model representation. *Reliability Engineering & System Safety*, 79(2), 187–193.
- [14] Saltelli, A., Annoni, P., Azzini, I., et al. (2010). Variance based sensitivity analysis of model output. design and estimator for the total sensitivity index. *Computer Physics Communications*, 181(2), 259–270.
- [15] Cukier, R., Schaibly, J., and Shuler, K. E. (1975). Study of the sensitivity of coupled reaction systems to uncertainties in rate coefficients. iii. analysis of the approximations. *The Journal of Chemical Physics*, 63(3), 1140–1149.
- [16] Saltelli, A., Tarantola, S., and Chan, K.-S. (1999). A quantitative model-independent method for global sensitivity analysis of model output. *Technometrics*, 41(1), 39–56.
- [17] Schoutens, W. (2012). *Stochastic processes and orthogonal polynomials*, vol. 146. Springer Science & Business Media.
- [18] Menga, E., Hernández, S., Moledo, S., et al. (2015). Nonlinear dynamic analysis of assembled aircraft structures with concentrated nonlinearities. *16th International Forum on Aeroelasticity and Structural Dynamics, IFASD2015*.

- [19] Hernández, S., Menga, E., Naveira, P., et al. (2017). Dynamic analysis of assembled structures with nonlinear joints. In *58th AIAA/ASCE/AHS/ASC Structures, Structural Dynamics, and Materials Conference, Grapevine, Texas, USA*.
- [20] Hernández, S., Menga, E., Moledo, S., et al. (2017). Optimization approach for identification of dynamic parameters of localized joints of aircraft assembled structures. *Aerospace Science and Technology*, (UNDER REVIEW).
- [21] Hernández, S., Menga, E., López, C., et al. (2017). An improved software for frequency domain analysis of assembled aircraft structures with local nonlinearities. *17th International Forum on Aeroelasticity and Structural Dynamics, IFASD2017*.

COPYRIGHT STATEMENT

The authors confirm that they, and/or their company or organization, hold copyright on all of the original material included in this paper. The authors also confirm that they have obtained permission, from the copyright holder of any third party material included in this paper, to publish it as part of their paper. The authors confirm that they give permission, or have obtained permission from the copyright holder of this paper, for the publication and distribution of this paper as part of the IFASD-2017 proceedings or as individual off-prints from the proceedings.